Meteorological Impacts of Forest Mortality due to Insect Infestation in Colorado

Christine Wiedinmyer*

Earth System Laboratory, National Center for Atmospheric Research,[+] Boulder, Colorado

Michael Barlage, Mukul Tewari, and Fei Chen

Research Applications Laboratory, National Center for Atmospheric Research,[+] Boulder, Colorado

Received 30 June 2011; accepted 28 October 2011

ABSTRACT: Physical characteristics of forests and other ecosystems control land–atmosphere exchanges of water and energy and partly dictate local and regional meteorology. Insect infestation and resulting forest dieback can alter these characteristics and, further, modify land–atmosphere exchanges. In the past decade, insect infestation has led to large-scale forest mortality in western North America. This study uses a high-resolution mesoscale meteorological model coupled with a detailed land surface model to investigate the sensitivity of near-surface variables to insect-related forest mortality. The inclusion of this land surface disturbance in the model increased in simulated skin temperature by as much as 2.1 K. The modeled 2-m temperature increased an average of 1 K relative to the default simulations. A latent to sensible heat flux shift with a magnitude of 10%–15% of the available energy in the forested ecosystem was predicted after the inclusion of insect infestation and forest dieback. Although results were consistent across multiple model configurations, the characteristics

[+] The National Center for Atmospheric Research is sponsored by the National Science Foundation.

* Corresponding author address: Christine Wiedinmyer, P.O. Box 3000, Boulder, CO 80307.
E-mail address: christin@ucar.edu

DOI: 10.1175/2011EI419.1

of forests affected by insect infestations must be better constrained to more accurately predict their impacts. Despite the limited duration of the simulations (one week), these initial results suggest the importance of including large-scale forest mortality due to insect infestation in meteorological models and highlight the need for better observations of the characteristics and exchanges of these disturbed landscapes.

KEYWORDS: Land-cover disturbance; Colorado; Forest mortality; WRF; Insect infestation; Bark beetles

1. Introduction

The characteristics of forests and other ecosystems, including albedo, emissivity, canopy conductance, and roughness length, are key parameters that control land–atmospheric exchanges of water and energy, and they partly dictate local and regional meteorology. Disturbances, such as fire or large-scale vegetation dieback, can dramatically alter these physical characteristics. For example, surface albedo can be changed significantly after a landscape has been burned (e.g., Liu et al. 2005; Amiro et al. 2006; Randerson et al. 2006; Myhre et al. 2005).

The importance of these impacts is highlighted by Running (Running 2008), who emphasizes the need to include land-cover disturbances, such as fire and forest dieback, in climate models to adequately account for changes in surface characteristics and carbon fluxes. The modification of physical land surface properties by disturbances can alter the surface–atmosphere exchanges of heat, water, and momentum and ultimately impact atmospheric processes such as the formation of clouds and precipitation through modifying the thermodynamic structures of the atmospheric boundary layer. Smaller surface roughness due to removal of the canopy overstory reduced sensible heat fluxes (HFX) during summer in the early and intermediate stages of postfire succession (Chambers et al. 2005). Reducing sensible heat fluxes increases surface soil temperatures, heat fluxes into the ground, and surface longwave radiation into the atmosphere (Liu et al. 2005; Viereck 1982). Wendt et al. (Wendt et al. 2007) observed an increase in sensible heat flux and boundary layer depth in burned tropical savanna in Australia. Chen et al. (Chen et al. 2001) illustrated the impacts of disturbed landscapes on atmospheric processes by representing a large burned area in a mesoscale model; the inclusion of the altered landscape caused an enhancement of the modeled convection over that area. Burned surfaces, with increased surface heating due to the reduction in surface albedo and soil moisture, can enhance atmospheric instability, increase the convective available potential energy, and augment local precipitation (Gallucci et al. 2011).

In the past decade, mountain pine beetle infestations have led to unprecedented forest mortality across the western mountain regions of North America (e.g., Hicke and Jenkins 2008). The forest dieback due to this insect infestation has been most pronounced in British Columbia, Canada, although large areas of forest mortality are observed throughout the western United States (Raffa et al. 2008; Hicke and Jenkins 2008). Forests killed by mountain pine beetles in British Columbia have been converted from a small net carbon sink to a large net carbon source (Kurz et al. 2008), and a study for the western United States showed that carbon stocks are altered in forests impacted by bark beetles differently than forests affected by stand-replacing wildfire and clear-cut harvesting (Pfeifer et al. 2010). These natural disturbances can significantly alter the physical and physiological properties (e.g., albedo, emissivity, roughness length, canopy resistance) of forests, which in turn affect land–atmospheric exchange, boundary layer structure, snow accumulation and ablation, and cloud characteristics and precipitation. For example, Boon (Boon 2007) examined the impact of mountain pine beetle infestation and subsequent canopy mortality on ground snow accumulation and ablation for 2005–06 and found a prolonged snowpack for a beetle-killed forest area.

To date, the impacts, if any, of large-scale insect disturbances on local and regional meteorology are unknown. Here, the effects of forest mortality from mountain pine beetle infestation in the central Rocky Mountains region of the United States on local near-surface meteorological variables are investigated. To determine the sensitivity of simulated local and regional-scale near-surface variables to large-scale forest changes, existing maps of forest mortality and insect infestation are used with a mesoscale meteorological model to perform sensitivity studies and examine the direct impacts of forest mortality on surface–atmosphere exchanges and near-surface variables. Although observations of the physical and physiological properties of beetle-killed forests are lacking, the sensitivity study here provides an evaluation of the importance of the inclusion of these landscapes in local predictions. Other modeling studies have investigated the sensitivity of meteorological predictions to land-cover characteristics (e.g., Zhang and Gao 2009; Chen et al. 2001; Gallucci et al. 2011) or the impact of forest mortality due to mountain pine beetle infestation on carbon exchange (Kurz et al. 2008; Pfeifer et al. 2010). Yet, this is the first such test of the sensitivity of the coupled Noah land surface model with the Weather Research and Forecasting (WRF) model to analyze the interactions between forest dieback and the atmosphere and their impacts on local meteorological variables. This study differs from other studies because of its regional focus on Colorado and the western United States, on the areas with identified bark beetle infestation.

2. Methodology

Mesoscale meteorology was simulated using the Advanced Research WRF model (ARW-WRF; Skamarock et al. 2007) version 3.0 over the western United States. The model was configured with three nested grids: (i) a large domain with 9-km grid spacing (303 by 262 grid cells; domain A), (ii) an intermediate domain with 3-km grid spacing (298 by 223 grid cells; domain B), and (iii) a small domain with 1-km grid spacing (391 by 323 grid cells; domain C) (Figure 1). The fine-resolution model domain (domain C) was chosen to encompass large areas of forest known to have experienced dieback due to insect infestation within Colorado. The WRF model was run with two-way coupling between the nested domains. The following WRF model physics options were used: the WRF single-moment three-class simple ice scheme, the Rapid Radiative Transfer Model for longwave radiation, the shortwave radiation schemes by Dudhia (Dudhia 1989), the Mellor–Yamada–Janjić (MYJ) planetary boundary layer (PBL) scheme (Janjić 1994), and the Noah land surface model (Chen and Dudhia 2001; Ek et al. 2003).

In this pilot sensitivity study, a relatively short, one-week period (8–14 June 2007) was chosen to represent fairly clear weather conditions for the central Rocky Mountains region. This one-week simulation served as a compromise between a

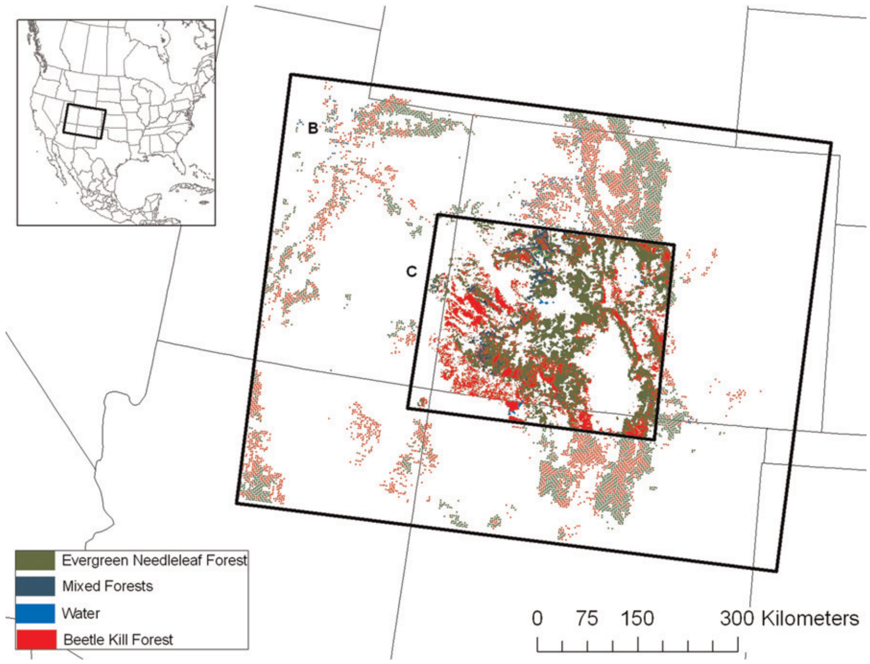

Figure 1. The intermediate 4-km model domain (domain B) and the small 1-km model domain (domain C). Forested areas (as defined by the MODIS LCT) are in green/dark blue. The areas assigned with forest mortality are in red.

computationally expensive monthly (or seasonal) simulations and a single case study. It was in accordance with typical 1–5-day numerical weather predictions and was considered a sufficient length to identify the magnitude of any changes in the predicted meteorology due to alterations in land-cover characteristics and to smooth any daily changes. Over the central Rocky Mountains region, the typical week featured diverse weather conditions including high pressure systems and clear-sky days (8–10 and 13 June 2007) and cold front passage (11–12 and 14 June 2007). A predominantly clear-sky case was chosen to best isolate any simulated changes in near-surface variables due to changes in land cover; the sensitivity of the output to periods of precipitation may have been more difficult to isolate. Future studies will investigate the longer-term, seasonal impacts of these large-scale forest diebacks across the western United States for cold and warm seasons; this study was completed to initially assess the relative strength of the impacts before more robust, expensive, and time-intensive studies are performed.

The WRF model simulations were executed starting with 1200 UTC 8 June 2007 and integrated for one week. The initial lateral boundary conditions were obtained from National Centers for Environmental Prediction (NCEP) Eta Data Assimilation System (EDAS)/North American Mesoscale (NAM) 212-grid (40 km) model analysis and were updated every 3 h. The soil moisture initial conditions were also taken from the EDAS/NAM. Two simulations with differing land surfaces were performed: 1) CONTROL simulation, using the land use/land cover defined by the Moderate Resolution Imaging Spectroradiometer (MODIS) land-cover-type product

(LCT; Friedl et al. 2002) and using the International Geosphere–Biosphere Programme (IGBP) land-cover classification system that provides 19 land-use/land-cover classifications at a 1-km spatial resolution, and 2) BEETLE simulation, using the U.S. Department of Agriculture Forest Service (USFS) 1997–2005 aerial survey data to identify areas of insect infestation and forest mortality. For the BEETLE simulation, infested areas with forest mortality identified using the USFS data replaced the default LCT data. Any areas with impacts as identified using the USFS dataset were assumed to have extensive forest mortality, and beetle-killed trees replaced the existing LCT forest classification (Figure 1, areas in red). This allowed for a realistic mapping of the spatial extent of insect infestation within the model domain. Although the areas identified by the survey data as infested by insects have differing levels of mortality, the worst-case scenario was chosen for this initial study to identify the maximum possible disturbance in the model and to determine if in fact these altered landscapes have a significant impact on meteorology at all. In domains B and C (Figure 1), about 47% and 40% of evergreen-forest pixels (8% and 14% of total pixels) are assigned as killed, respectively. The following vegetation parameters of the beetle-killed forest class in WRF–Noah were changed (from the default summer forest values in the parenthesis): albedo increased to 0.15 (0.1), green vegetation fraction reduced to 0.3 (0.7), active transpiration root zone reduced to 10 cm below the ground (200 cm), minimum canopy resistance increased to 600 m s^{-1} (125 m s^{-1}), and green leaf area index (LAI) reduced to 1 (4). The chosen model modifications are intended to capture zero-order characteristics (less green leaves, higher reflectivity, and low canopy transpiration) of the new, dead forest classification. We recognize that the selection of these parameters is highly uncertain because of the lack of available direct observations of the above parameters for these types of landscapes. However, the values used here follow basic logical assumptions; such a parameter modification may still present maximized effects.

3. Results

Two 7-day simulations (CONTROL and BEETLE) were performed for the three nested domains for 8–14 June 2007. Meteorological surface stations provided observations within the innermost model domain (domain C) for evaluation of the model simulations. In addition to evaluation with surface observations, the MODIS land surface temperature (LST) product (MOD11; Wan et al. 2002), a daily global product with a 1-km spatial resolution, was used to further evaluate predicted skin temperatures. Data from MODIS sensors on both *Aqua* and *Terra* satellites were used and provided four comparison points in each diurnal cycle. An initial comparison between the CONTROL and the BEETLE simulation skin temperature results, and the observed skin temperature from the MODIS instruments over the model simulation period is shown in Figure 2.

For those grid cells assigned forest land cover, the CONTROL simulation showed a consistent negative bias in afternoon skin temperature when compared to the MODIS skin temperature observations for all days except for 11 June, with a weekly averaged mean bias of −1.7 K (Table 1). For these comparisons, hourly WRF output was interpolated to the time of the MODIS overpasses. Inclusion of the forest dieback (BEETLE) improved this result; the mean bias in hourly

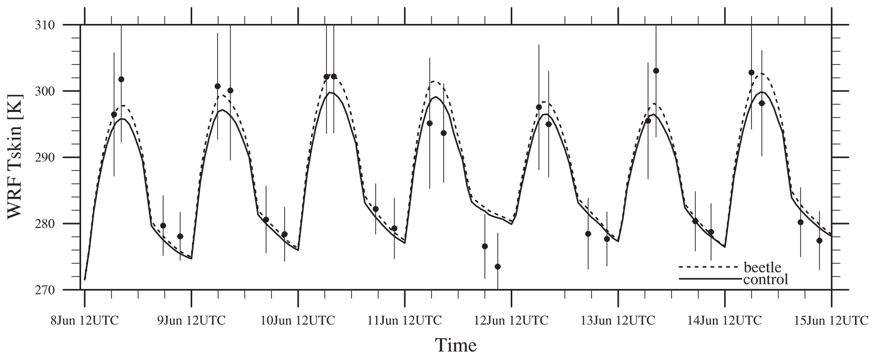

Figure 2. Modeled skin temperature compared to the MODIS LST for a 7-day simulation starting at 1200 UTC 8 Jun. The dashed line is from grids with beetle-killed trees, and solid lines are from the same locations in the control simulation but with no beetle effects. Dots are the mean MODIS LST observations with vertical lines of ±one standard deviation in LST.

afternoon skin temperature for the 7-day simulation was reduced to 0.4 K (Table 1). This is solely the result of the changed land surface parameters assigned to the beetle-killed forests: albedo, green vegetation fraction, active transpiration root zone, minimum canopy resistance, and green leaf area index. The improvement in simulated skin temperatures suggests that the inclusion of areas with forest mortality are located correctly within the model domain; however, the continued bias highlights the uncertainty in both the observed MODIS skin temperatures and the parameters assigned to the dead forests in the WRF–Noah simulations.

The simulated average midafternoon (1700–2200 UTC) skin temperatures in the grid cells with beetle-killed forests were 2.1 K greater than the undisturbed evergreen needleleaf forest grid cells (Table 2). In a healthy forest, significant energy is transported from the surface to the atmosphere in the form of evapotranspiration. After beetle infestation, the surface energy balance is maintained by increasing the surface skin temperature and therefore increasing both surface sensible heat flux and longwave radiative flux sufficiently to balance the loss of latent heat flux (QFX). Qualitatively, this result is comparable to findings from an observational study of large-scale forest mortality due to insect infestation in the Czech Republic. Using Landsat thermal imagery for 1987 and 2002, Hais and Kucera (Hais and Kucera 2008) observed a 3.5-K increase in surface temperature in a spruce forest in the Czech Republic that had been impacted by bark beetles, compared to the same forest before the disturbance took place. Differences in forest structure and species

Table 1. Skin temperature bias (K) from the two model simulations when compared to the average of the two daytime MODIS LST data for those model grids with forest mortality. Note that hourly model results were interpolated to the MODIS overpass times (*Terra* at ~1730 UTC and *Aqua* at ~2030 UTC).

	8 Jun	9 Jun	10 Jun	11 Jun	12 Jun	13 Jun	14 Jun	Mean
CONTROL	−3.9	−3.9	−2.7	3.7	−0.4	−3.2	−1.5	−1.7
BEETLE	−2.0	−1.8	−0.1	6.1	1.5	−1.8	1.1	0.4

Table 2. Difference (BEETLE − CONTROL) in simulated meteorological variables only over areas with forest mortality for 1700–0000 UTC each day (except for skin temperature, which is for 1700–2200 UTC each day).

	8 Jun	9 Jun	10 Jun	11 Jun	12 Jun	13 Jun	14 Jun	Mean
Skin temp (K)	1.8	2.1	2.6	2.4	1.8	1.5	2.6	2.1
T-2meter (K)	0.7	0.8	1	0.9	0.7	0.7	1.1	0.8
HFX (W m^{-2})	151	108	127	114	91	82	125	114
QFX (W m^{-2})	−115	−115	−135	−121	−94	−97	−130	−115
PBLH (m)	70	100	180	133	102	107	185	125

distributions between the forest studies in the Czech Republic and the forests in the western United States, as well as differences in the level of forest dieback, could explain some of the discrepancy between the two results. Yet, both showed similar trends, and it should be noted that, although forests in western United States and spruce forests in the Czech Republic are not identical, they are both labeled as needleleaf evergreen forests within models and assigned similar, if not identical, physical parameterizations.

The simulated surface–atmosphere exchanges and resulting near-surface variables were sensitive to the inclusion of areas of forest mortality over the entire domain; for the model grid cells identified as beetle-killed, the near-surface variables are substantially different than they are for grid cells assigned to the default forest type. Figure 3 shows the weeklong daytime-averaged profile of several modeled variables for all grid cells identified as evergreen needleleaf forests (solid line) and all grid cells assigned as dead forests in the BEETLE case (dashed line). The daytime-averaged (1700–0000 UTC) difference in the 2-m temperatures (T-2meter; BEETLE − CONTROL) ranged from 0.7 to 1.1 K, with an average increase of 0.8 K (Table 2) in grid cells where forest mortality was assigned. The 24-h average differences ranged from 0.42 to 0.74 K. Increases in air temperatures are expected because of the increased skin temperatures and increased sensible heat flux.

For grid cells in which forest dieback was assigned, daytime sensible heat flux increased on average by 114 W m^{-2} (82–151 W m^{-2}) over the simulation, and daytime latent heat fluxes decreased on average by 115 W m^{-2} (94–135 W m^{-2}) (Table 2). This modeled flux shift in sensible and latent heat between the BEETLE and the CONTROL cases is equivalent to approximately 10%–15% of the available energy in that ecosystem. The decreased latent heat flux and associated increased sensible heat flux lead to a domain-wide decrease in atmospheric moisture. The largest decreases in latent heat flux are located in areas impacted by beetle-induced mortality where less water is exchanged between the biosphere and the atmosphere. However, latent heat increases are observed in other model grids without the beetle disturbance. As latent heat fluxes decrease over the beetle-infested region, the near-surface atmosphere downwind is drier and the potential for larger evapotranspiration in the unaffected regions increases. The spatial distribution of these changes is not uniform, however, because they are impacted by not only the changes in latent heat flux but also downwind mesoscale forcings, topography, and land cover.

Most of the latent heat flux occurs during the daytime; the integrated daytime latent heat is ~75%–80% of the daily total. The total daily latent heat flux

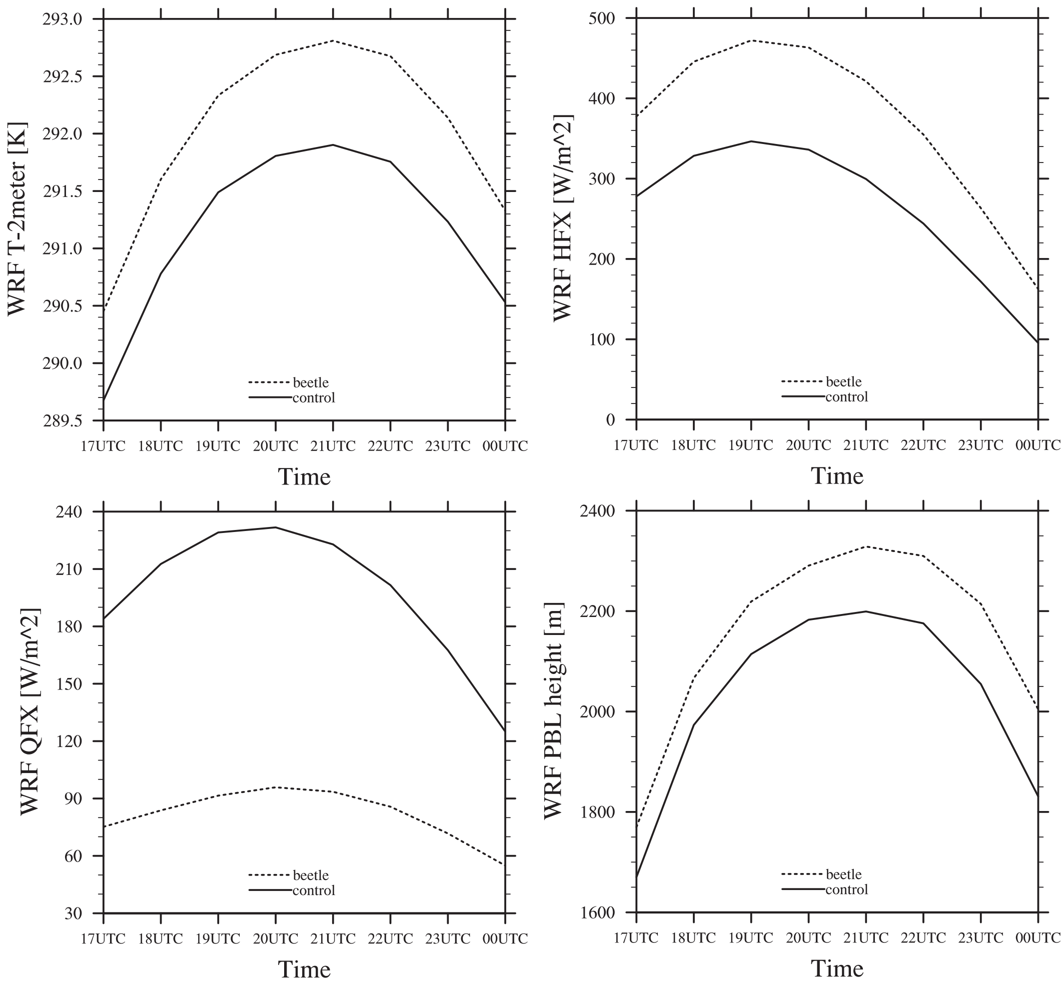

Figure 3. Daytime-simulated output of T-2meter, HFX, QFX, and PBLH from CONTROL (solid lines) and BEETLE (dashed lines) averaged for the weeklong simulation. Results are only for areas identified with forest mortality.

reduction over the 7-day simulation ranged from 36 to 55 W m^{-2}, suggesting that, because of decreased evapotranspiration, approximately 1.2–1.9 mm of water remains in the soil daily in those grid cells that are impacted by forest mortality. This soil water cannot accumulate indefinitely and will eventually result in increased direct soil evaporation and subsurface runoff.

The difference in the daily averaged planetary boundary layer height (PBLH) for the areas identified with forest mortality (BEETLE − CONTROL) ranged from 70 to 185 m, with a weeklong average of 125 m. The average daily boundary layer height reached approximately 2200 m. The largest increases are observed above the areas impacted by the beetle-infested forests. Yet, changes are observed throughout the domain. Increases in turbulent kinetic energy and boundary layer instability are also expected because they are directly related to increases in PBLH.

To test the robustness of the results relative to choice of model parameterization, additional WRF simulations were conducted using the Yonsei University (YSU) planetary boundary layer scheme (Hong et al. 2006). As expected, specific results of the model depended on the PBL scheme used in WRF, and the output from the CONTROL simulations with the YSU scheme and those using the MYJ scheme differed from one another significantly. However, for the additional simulations using the YSU scheme, the differences of near-surface temperature, humidity, wind speed (not discussed here), surface fluxes, and PBLH between evergreen-forest grid cells and beetled-killed-tree grid cells are very similar to those between CONTROL and BEETLE simulations. For example, the difference in mean skin temperature at 2000 UTC (BEETLE − CONTROL) for the simulation using the MYJ parameterization was 1.98 K; this result was 1.96 K for the simulations using the YSU parameterization. Furthermore, the differences in the hourly averaged sensible heat flux of the model simulations using MYJ and YSU was the same: 125 W m^{-2}. Hence, the WRF simulation results show that the model (WRF–Noah) is robust and sensitive to forest disturbance, regardless of the schemes chosen.

4. Conclusions

This paper presents the results of a sensitivity study using the coupled WRF–Noah model, which demonstrate that local land surface interactions and simulated meteorology are sensitive to changes in surface characteristics caused by beetle infestation and forest mortality. Surface skin temperatures in areas of bark beetle infestation and forest mortality are increased by an average of 2.1 K compared to undisturbed evergreen needleleaf forests. Simulated hourly boundary layer heights increased up to 65% in model grids that include these land-cover impacts.

The results observed from this sensitivity study show that changing the land surface properties to simulate large-scale forest mortality from bark beetles can alter simulated near-surface variables that have influence on local and regional meteorology. Further, these results can have significant impacts on modeled atmospheric chemistry, because the depth of the mixed layer will in part control simulated gas and particle concentrations. Modeled boundary layer depth is a key factor in determining the concentrations of atmospheric trace gases, which drives their transport and dispersion. Additionally, changes in air temperature by 2 K can dramatically increase biogenic volatile organic compound emissions of the remaining and nearby trees, because these emissions are controlled by temperature (e.g., Guenther et al. 1995). As highlighted by Running (Running 2008), land-cover disturbances can impact land surface exchanges and ultimately weather, climate, and chemistry. Note that the land surface properties of beetle-killed trees in all stages of decay are not well constrained and the physical parameterizations chosen for this study were assigned based on assumptions and a worst-case scenario. Although the differences in the surface skin temperature between beetle-killed trees and natural forests agreed, to a large degree, with differences in MODIS skin temperature observations, the interpretation of these sensitivity results needs to be cautious. Based on the results and the potential impacts that these disturbances could potentially have, more observations of the vegetation parameters in disturbed areas are necessary so that these processes can be better included in regional and global models that simulate weather, climate, and chemistry. These results could impact local weather predictions in regions characterized by high forest mortality. As the outbreaks continue and more forests die back as a result, this type of disturbance should be considered when modeling local and regional meteorology and chemistry in the western North America.

Acknowledgments. Any opinions, findings, and conclusions expressed in this material are those of the authors and do not necessarily reflect the views of the funding agencies. This study was supported by the NSF/NCAR Bio-Hydro-Atmosphere Interactions of Energy, Aerosols, Carbon, H2O, and Organics & Nitrogen (BEACHON) program.

References

Amiro, B. D., and Coauthors, 2006: The effect of post-fire stand age on the boreal forest energy balance. *Agric. For. Meteor.,* **140** (1–4), 41–50.

Boon, S., 2007: Snow accumulation and ablation in a beetle-killed pine stand in northern interior British Columbia. *BC J. Ecosyst. Manage.,* **8** (3), 1–13.

Chambers, S. D., J. Beringer, J. T. Randerson, and F. S. Chapin III, 2005: Fire effects on net radiation and energy partitioning: Contrasting responses of tundra and boreal forest ecosystems. *J. Geophys. Res.,* **110,** D09106, doi:10.1029/2004JD005299.

Chen, F., and J. Dudhia, 2001: Coupling an advanced land surface–hydrology model with the Penn State–NCAR MM5 modeling system. Part I: Model implementation and sensitivity. *Mon. Wea. Rev.,* **129,** 569–585.

——, T. T. Warner, and K. Manning, 2001: Sensitivity of orographic moist convection to landscape variability: A study of the Buffalo Creek, Colorado, flash flood case of 1996. *J. Atmos. Sci.,* **58,** 3204–3223.

Dudhia, J., 1989: Numerical study of convection observed during the winter monsoon experiment using a mesoscale two-dimensional model. *J. Atmos. Sci.,* **46,** 3077–3107.

Ek, M. B., K. E. Mitchell, Y. Lin, E. Rogers, P. Grunmann, V. Koren, G. Gayno, and J. D. Tarpley, 2003: Implementation of Noah land surface model advances in the National Centers for Environmental Prediction operational mesoscale Eta model. *J. Geophys. Res.,* **108,** 8851, doi:10.1029/2002JD003296.

Friedl, M. A., and Coauthors, 2002: Global land cover mapping from MODIS: Algorithms and early results. *Remote Sens. Environ.,* **83** (1–2), 287–302.

Gallucci, J., L. Tryhorn, A. Lynch, and K. Parkyn, 2011: On the meteorological and hydrological mechanisms resulting in the 2003 post-fire flood event in Alpine Shire, Victoria. *Aust. Meteor. Oceanogr. J.,* **61,** 31–42.

Guenther, A., and Coauthors, 1995: A global model of natural volatile organic compound emissions. *J. Geophys. Res.,* **100,** 8873–8892.

Hais, M., and T. Kucera, 2008: Surface temperature change of spruce forest as a result of bark beetle attack: Remote sensing and GIS approach. *Eur. J. For. Res.,* **127,** 327–336.

Hicke, J. A., and J. C. Jenkins, 2008: Mapping lodgepole pine stand structure susceptibility to mountain pine beetle attack across the western United States. *For. Ecol. Manage.,* **255** (5–6), 1536–1547.

Hong, S.-Y., Y. Noh, and J. Dudhia, 2006: A new vertical diffusion package with an explicit treatment of entrainment processes. *Mon. Wea. Rev.,* **134,** 2318–2341.

Janjić, Z. I., 1994: The step-mountain Eta coordinate model: Further developments of the convection, viscous sublayer, and turbulence closure schemes. *Mon. Wea. Rev.,* **122,** 927–945.

Kurz, W. A., C. C. Dymond, G. Stinson, G. J. Rampley, E. T. Neilson, A. L. Carroll, T. Ebata, and L. Safranyik, 2008: Mountain pine beetle and forest carbon feedback to climate change. *Nature,* **452,** 987–990.

Liu, H., J. T. Randerson, J. Lindfors, and F. S. Chapin III, 2005: Changes in the surface energy budget after fire in boreal ecosystems of interior Alaska: An annual perspective. *J. Geophys. Res.,* **110,** D13101, doi:10.1029/2004JD005158.

Myhre, G., Y. Govaerts, J. M. Haywood, T. K. Berntsen, and A. Lattanzio, 2005: Radiative effect of surface albedo change from biomass burning. *Geophys. Res. Lett.,* **32,** L20812, doi:10.1029/2005GL022897.

Pfeifer, E. M., J. A. Hicke, and A. J. H. Meddens, 2010: Observations and modeling of aboveground tree carbon stocks and fluxes following a bark beetle outbreak in the western United States. *Global Change Biol.,* **17,** 339–350, doi:10.1111/j.1365-2486.2010.02226.x.

Raffa, K. F., B. H. Aukema, B. J. Bentz, A. L. Carroll, J. A. Hicke, M. G. Turner, and W. H. Romme, 2008: Cross-scale drivers of natural disturbances prone to anthropogenic amplification: The dynamics of bark beetle eruptions. *Bioscience,* **58,** 501–517.

Randerson, J. T., and Coauthors, 2006: The impact of boreal forest fire on climate warming. *Science,* **314,** 1130–1132.

Running, S. W., 2008: Ecosystem disturbance, carbon, and climate. *Science,* **321** (5889), 652–653.

Skamarock, W. C., J. B. Klemp, J. Dudhia, D. O. Gill, D. M. Barker, W. Wang, and J. G. Powers, 2007: A description of the advanced research WRF version 2. NCAR Tech. Note NCAR/TN-468+STR, 88 pp.

Viereck, L. A., 1982: Effects of fire and firelines on active layer thickness and soil temperatures in interior Alaska. *Proc. Fourth Canadian Permafrost Conf.,* Calgary, Canada, Natural Resource Council of Canada, 123–135.

Wan, Z., Y. Zhang, Q. Zhang, and Z.-L. Li, 2002: Validation of the land-surface temperature products retrieved from Terra Moderate Resolution Imaging Spectroradiometer data. *Remote Sens. Environ.,* **83** (1–2), 163–180.

Wendt, C. K., J. Beringer, N. Tapper, and L. B. Hurley, 2007: Local boundary-layer development over burnt and unburnt tropical savanna: An observational study. *Bound.-Layer Meteor.,* **124,** 291–304.

Zhang, H. Q., and X. J. Gao, 2009: On the atmospheric dynamical responses to land-use change in East Asian monsoon region. *Climate Dyn.,* **33** (2–3), 409–426.